Bioresource Technology Reports 18 (2022) 101045

Contents lists available at ScienceDirect

Bioresource Technology Reports

journal homepage: www.sciencedirect.com/journal/bioresource-technology-reports

Insights into the removal of lithium and molybdenum from groundwater by adsorption onto activated carbon, bentonite, roasted date pits, and modified-roasted date pits

Ayesha Y. Ahmad [a], Mohammad A. Al-Ghouti [a,*], Majeda Khraisheh [b], Nabil Zouari [a]

[a] Environmental Science Program, Department of Biological and Environmental Sciences, College of Arts and Sciences, Qatar University, P.O. Box 2713, Doha, Qatar
[b] Department of Chemical Engineering, College of Engineering, Qatar University, P.O. Box 2713, Doha, Qatar

ARTICLE INFO

Keywords:
Groundwater
Agricultural waste
Adsorption isotherm models
Thermodynamics

ABSTRACT

This study investigated the removal of lithium (Li) and molybdenum (Mo) from groundwater using activated carbon, bentonite, roasted date pits, and modified-roasted date pits as adsorbents under different experimental parameters including pH, initial concentration, and temperature. Various adsorption isotherm models were used to determine the best-fit model for the obtained experimental data. The negative values of Gibbs energy (ΔG°) indicated a spontaneous and favorable adsorption process of the adsorption at high temperatures. The positive entropy values (ΔS°) that controlled the adsorption process suggested the possibility of some structural changes or readjustments in the adsorbate–adsorbent complex. The adsorption efficiency of Li increases at 35 °C using the four adsorbents. At 35 °C, the maximum adsorption efficiency reached 95% for AC, 94% using MDPs, 63% using bentonite, and 38% using RDPs. The modified-roasted date pits showed the highest adsorption of Mo in all real groundwater samples. The adsorption of Mo increased with the increase in concentrations, and its maximum removal at 25 °C was 80%.

1. Introduction

In Qatar, as a semi-arid country, natural renewable water resources are limited to rainfall and groundwater. However, depleting these resources each year will lead to various challenges. As a result of the increased consumption and population, the demand for fresh clean water will increase which in turn will lead to unsustainable status and regional water crisis. Since precipitation rates are low and are not sufficient to fulfill the water demand, Qatar can rely on groundwater aquifers as the only renewable water source (Wahib et al., 2022). However, overexploitation of groundwater can cause deterioration of the groundwater and decrease its quality making it the most important water security concern. Mallick et al. (2018) discussed various factors that can affect the quality of groundwater namely, sewage, spills, and leaching of fertilizers. Moreover, according to Etteieb et al. (2015), the quality and quantity of groundwater are negatively affected by various factors including the high development of agriculture, increased freshwater demand, vast pumping of groundwater, and rapid urbanization (Al-Shidi, 2014). Management of water resources is a challenging practice because of the limited water accessibility and availability. Various natural and anthropogenic activities such as saline water intrusion, mineral weathering, and high evaporation rates negatively affect the groundwater making it unsuitable for any domestic or agricultural use (El-Alfy et al., 2017; Al-Shidi, 2014).

In Qatar, it is known that groundwater resources have the most availability and accessibility, therefore, the development of novel, cost-efficient and eco-friendly treatment approaches for the improvement of its quality. This will aid in the enhancement of water security as well as resolving the groundwater yield issue with better quantity and quality. Metals elimination from the aqueous medium can be achieved by various conventional methods each with its own benefits and drawbacks. These techniques include chemical precipitation, sorption, advanced oxidation, and others (Younas et al., 2021). According to Ahmad et al. (2011), ion exchange and membrane technologies are not cost-efficient but have high selectivity toward metals. Moreover, adsorption is one of the main techniques applied for metal removal from groundwater (Huang et al., 2016). It is known to be cost-efficient, environmentally friendly, simple in design, easy to operate, and it can be used for the removal of contaminants of low to moderate levels (Yang et al., 2009; Karnib et al., 2014; Amin et al., 2016).

* Corresponding author.
E-mail address: mohammad.alghouti@qu.edu.qa (M.A. Al-Ghouti).

https://doi.org/10.1016/j.biteb.2022.101045
Received 22 January 2022; Received in revised form 3 April 2022; Accepted 4 April 2022
Available online 9 April 2022

Our preliminary research has shown that groundwater has various metals such as lithium (Li) and molybdenum (Mo), which may exceed the permissible limits. The mean values in 41 wells of groundwater aquifers in Qatar were found to be 0.120 mg/L and 0.0538 mg/L, respectively (Ahmad et al., 2020). Li and Mo are of great concern as they can potentially induce toxicity to agricultural products if it exceeds the permissible levels (Ahmad et al., 2020). The high demand for Li in many commercial applications has increased research on its recovery over the past decades (Sun et al., 2018). Moreover, in Qatari groundwater, Mo can exist as a result of the oil and gas processing industry, which is used in the desulfurization process as a catalyst (Kuiper et al., 2015). Additionally, Mo is utilized in pigments production, fertilizers, corrosion inhibitors, and lubricants (IMOA, 2018).

Adsorption is an efficient technique for removing metal ions from solutions (Wang et al., 2017). Adsorption is known to overcome any associated challenges with the different treatment methods as it is feasible, simply operated, cost-efficient, and environmentally friendly. An activated carbon surface can adsorb metals due to oxygen-containing functional groups so that Li and Mo ions could be adsorbed by the electrostatic interaction of positive and negative charges. However, there is a lack of thermodynamics and kinetics of Li and Mo adsorption in the aqueous phase (Zhang et al., 2017). Hence, the development of an effective Li and Mo removal method from an aqueous solution is crucial.

Moreover, various adsorbents are well-established to remediate different pollutants from the aqueous medium, such as activated carbon and chitosan, which undergo different modifications to enhance their adsorptive characteristics. However, the high cost and utilization of harmful and toxic chemicals are the drawbacks of this process. Thus, researchers are looking for cost-efficient, natural-based and effective adsorbent that does not negatively affect the environment. A great adsorptive potential is demonstrated by date pits toward various pollutants because of their composition and structure. Since Qatar is one of the world's largest producers of dates, each year it generates massive amounts of date pits as agricultural waste. Thus, date pits demonstrate a sustainable, cost-efficient, eco-friendly, and effective adsorbent for the removal of Li and Mo from groundwater (Al-Absi et al., 2021). Therefore, the objectives of this study are (i) to produce modified-date pits by using mercapto-acetic acid, (ii) to evaluate the adsorption capacity of activated carbon, bentonite clay, date pits, and modified date pits in removing Li and Mo from synthetic and real groundwater, and (iii) to compare the adsorption of Li and Mo in different solutions such as single adsorbate solution, and real groundwater solution at 25°C.

2. Methodology

In the current study, solid-liquid adsorption is described, where the solid phase is called adsorbent and the liquid phase (groundwater) contains the adsorbates. The adsorption of Li and Mo is conducted using a lithium chloride/sodium molybdate solution stock solution and using real groundwater samples. The adsorption process involves different stages starting from the synthesis of adsorbents, optimization, and design of the adsorption process.

2.1. Adsorbent collection, preparation, modification, and characterization

Four different adsorbents were used to investigate the removal efficiency of Li and Mo from groundwater, namely commercial bentonite, activated carbon (AC), roasted date pits (RDPs) obtained from the Qatari date fruit *Phoenix dactylifera* L. from local markets, in addition to one modification that was applied to the RDPs to obtain the fourth adsorbent denoted as modified date pits (MDPs). In both adsorbents RDPs and MDPs, the only used part was the hard pit. Table 1 shows the surface area and pore size for different adsorbents. To obtain RDPs as an adsorbent, the process started with rinsing the date pits with deionized water and drying them for 2 h at 65 °C, followed by roasting them at 130 °C for 3 h. The next step was grounding the obtained RDPs with continuous washing with deionized water. After that, the samples were kept drying overnight at 100 °C. Finally, the obtained RDPs were sieved to obtain 0.25mm–0.125 mm particle size to be used as an adsorbent. In the current study, a proper surface modification method for the cost-efficient, green, and energy-saving adsorption processes was adopted. The first modification step was H_2SO_4 (100 mL, 98% w/w) modification. The second step was NaOH (200 mL, 1 M) modification to add hydroxyl functional groups, while the last step was mercaptoacetic acid ($C_2H_2O_2S$) (1 M) modification to change the abundant hydroxyl groups to mercapto groups, also known as a thiol group or a sulfhydryl group (–SH), which showed significant metal removal from water (Shafiq et al., 2019; Amin et al., 2016; Yadav et al., 2013). Finally, the obtained product was filtered, washed with deionized water, centrifuged, and dried overnight at 100 °C. Moreover, Brunauer Emmett Teller (BET) analysis of the used adsorbents was obtained and shown in Table 1.

Table 1
Brunauer Emmett Teller (BET) surface area parameters for the different adsorbents used in this study.

Parameters	Activated carbon	Bentonite	Roasted date pits	Modified roasted date pits
Surface area (m^2/g)	179	34.7	28.4	29.7
Single point total pore volume (cm^3/g)	0.165	0.187	0.0837	0.0980
Single point adsorption microporous volume (cm^3/g)	0.0780	0.0146	0.0100	0.0140
Single point average pore radius (nm)	1.88	10.8	5.7	6.31

2.2. Optimization and design of the adsorption process

The operating conditions of adsorption processes can be optimized to maximize the adsorbent efficiency to remove pollutants and reduce operational costs. Adsorption efficiency in treating groundwater is a function of different parameters namely pH, temperature, and initial adsorbate concentration. A 0.05 g of the adsorbent (bentonite, AC, RDPs, and MDPs) were added to 50 mL of lithium chloride/sodium molybdate solution of different initial concentrations (10 to 100 mg/L) under various pH values (2, 4, 6, 8, and 10) as well as various temperatures (25 °C, 35 °C, and 45 °C). The solutions were placed in acidified glass bottles with continuous shaking at 165 rpm for 24 h at the temperature-controlled shaker of different temperatures as mentioned previously (25 °C, 35 °C, and 45 °C). Then, filtration was done for all samples using membrane filters of 0.2 μm and the concentration of both Li and Mo was measured by using inductively coupled plasma mass spectrometry (ICP-MS), using US-EPA 200.8 method.

2.3. Adsorption isotherms and thermodynamic studies

Adsorption isotherm models can describe the relationship between the adsorption capacity and concentration at equilibrium and constant temperature. Therefore, four different models namely, Langmuir, Freundlich, Dubinin–Radushkevich, and Temkin adsorption isotherm models were utilized to investigate the best-fit model to the equilibrium data. Fig. 1 represents the parameters of the four models. Furthermore, thermodynamic studies are highly important for the interpretation of the adsorption process in terms of favourability, spontaneity, endothermic or exothermic. Thus, Gibb's free energy change (ΔG°), standard enthalpy change (ΔH°), and standard entropy change (ΔS°) are calculated through the following equations:

$$\Delta G^\circ = -RT\, lnb \quad (1)$$

$$\Delta G^\circ = \Delta H^\circ - T\Delta S^\circ \quad (2)$$

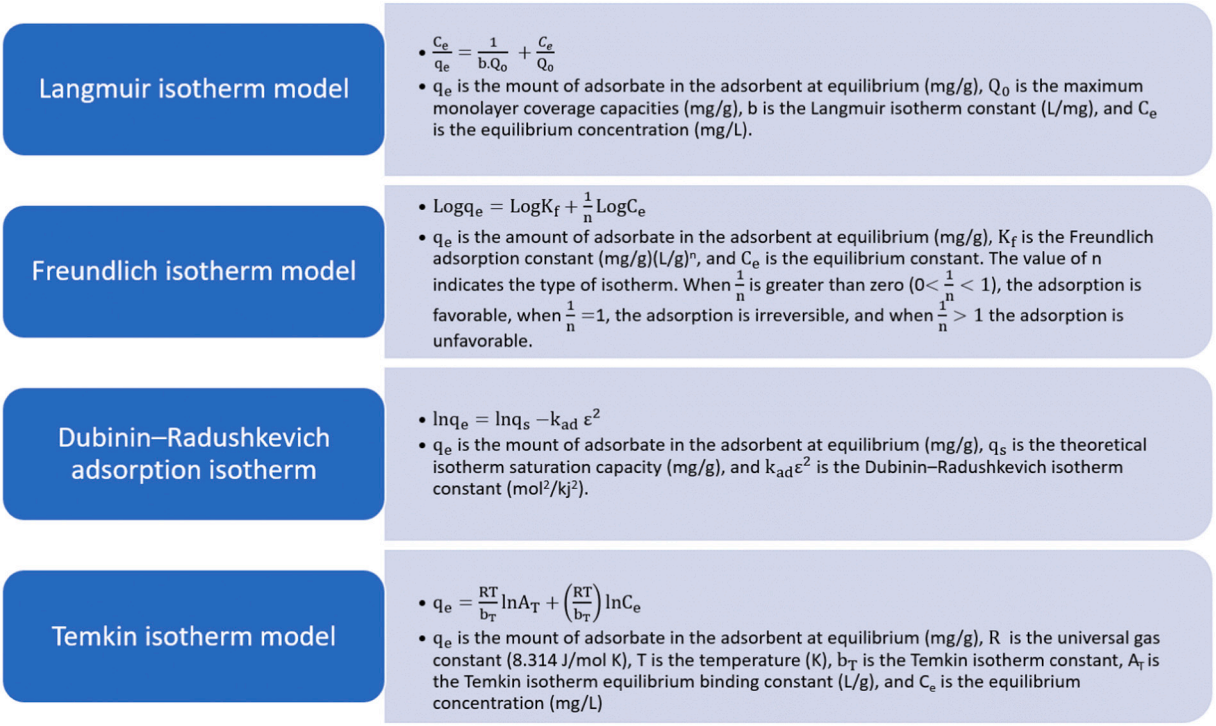

Fig. 1. Different adsorption isotherm models.

Where R is the gas constant (8.314 J/mol K), T is the temperature in Kelvin (K), and *b* is the Langmuir constant.

2.4. Statistical analysis

Since the experiments were factorial and completely randomized design (CRD) was the experimental design of the experiments, analysis of variance (ANOVA) for 2 factors was used to assist the relationship between the initial concentration and temperature. However, single-factor ANOVA was utilized for the effect of pH experiments. Chi-squared test (χ^2) and the coefficient of determination (R^2) were used to investigate the best-fit adsorption isotherm model.

3. Results and discussion

3.1. Physicochemical properties of Li and Mo

Adsorption depends on the pollutant adsorption onto the surface of the adsorbent (Shafiq et al., 2019). Adsorbate-adsorbent is attracted by various forces, including ion exchange, chemical bonding, Van der Waals forces, and hydrogen bonding (Ahmad et al., 2011). Moreover, the chemisorption process is an irreversible process that requires high temperature and occurs as a monolayer form, on the other hand, physisorption is a reversible process that does not require high temperature and occurs as a mono/multilayer form (Shafiq et al., 2019). To find a possible attractive site between adsorbate ions (Li and Mo) and adsorbents, characteristic properties such as crystal radius and equilibrium constants for adsorbate ions are important. According to Shannon (1976), the crystal radius of Li and Mo is 0.68 and 2.70, the hydration radius is 2.38 and 4.06 (Wang and Weinstock, 2012), the hydrolysis constant is 13.6 and 0.9 (Nagul et al., 2015), and the Pauling electronegativity is 0.912 and 2.16 (Daniel and Harris, 2011), respectively.

3.2. Effect of pH

3.2.1. Effect of pH in Li adsorption

The value of pH of the solution is a crucial parameter for the adsorption of metals from an aqueous solution since it determines the concentration of hydrogen ions and hydroxyl ions (Al-Ghouti et al., 2017). Therefore, different pH values were investigated in this study to determine their effect on the adsorption of Li and Mo from an aqueous medium by various adsorbents. The adsorption capacity is affected by the changes in the pH value as it causes a change in the functional groups to charge that is present on the adsorbent's surface. Fig. 2A illustrates the adsorption efficiency of Li onto the four used adsorbents, namely bentonite, AC, RDPs, and MDPs. It is illustrated that the Li optimum pH value in which the highest removal was achieved at pH 6 for RDPs, pH 8 for MDPs, and pH 4 for AC. It can be observed that the maximum removal efficiency of Li by bentonite and AC was 12.65% and 14.05% under acidic conditions at pH 2 and pH 4, respectively. However, the maximum adsorption percentage of Li by RDPs, and MDPs under alkaline conditions at pH 6 and pH 8 with removal percentages of 15.45%, and 14.6% respectively, while bentonite removal efficiency was 12.2% at pH 8. It is worth mentioning that the surface functional groups can be protonated at a low pH value causing the formation of a positive charge on the surface, however, the surface will become ionic and lose its protons at a high pH value (Heibati et al., 2014). This can be attributed to the increased number of OH^- ions with increasing the value of pH and the density of the negative charged binding sites that electrostatically attract Li^+ cations. While the decrease of Li adsorption onto RDPs, MDPs at low pH could be due to the competition between H^+ ions and Li ions for the adsorption sites, thus the adsorbed capacity of Li^+ decreases. Moreover, since H^+ ions concentration increases at low pH, these ions might desorb the previously bound metals back into the solution (Wahib et al., 2022). However, the increase of Li^+ adsorption by AC and bentonite at low pH could be due to the attraction between the chloride ions at the adsorption sites with Li^+ ions. The decrease of Li adsorption by AC at high pH could be explained by the electrostatic repulsion between the negatively charged species and the surface of the adsorbent. Furthermore, the surface charge of the adsorbent could be disturbed by

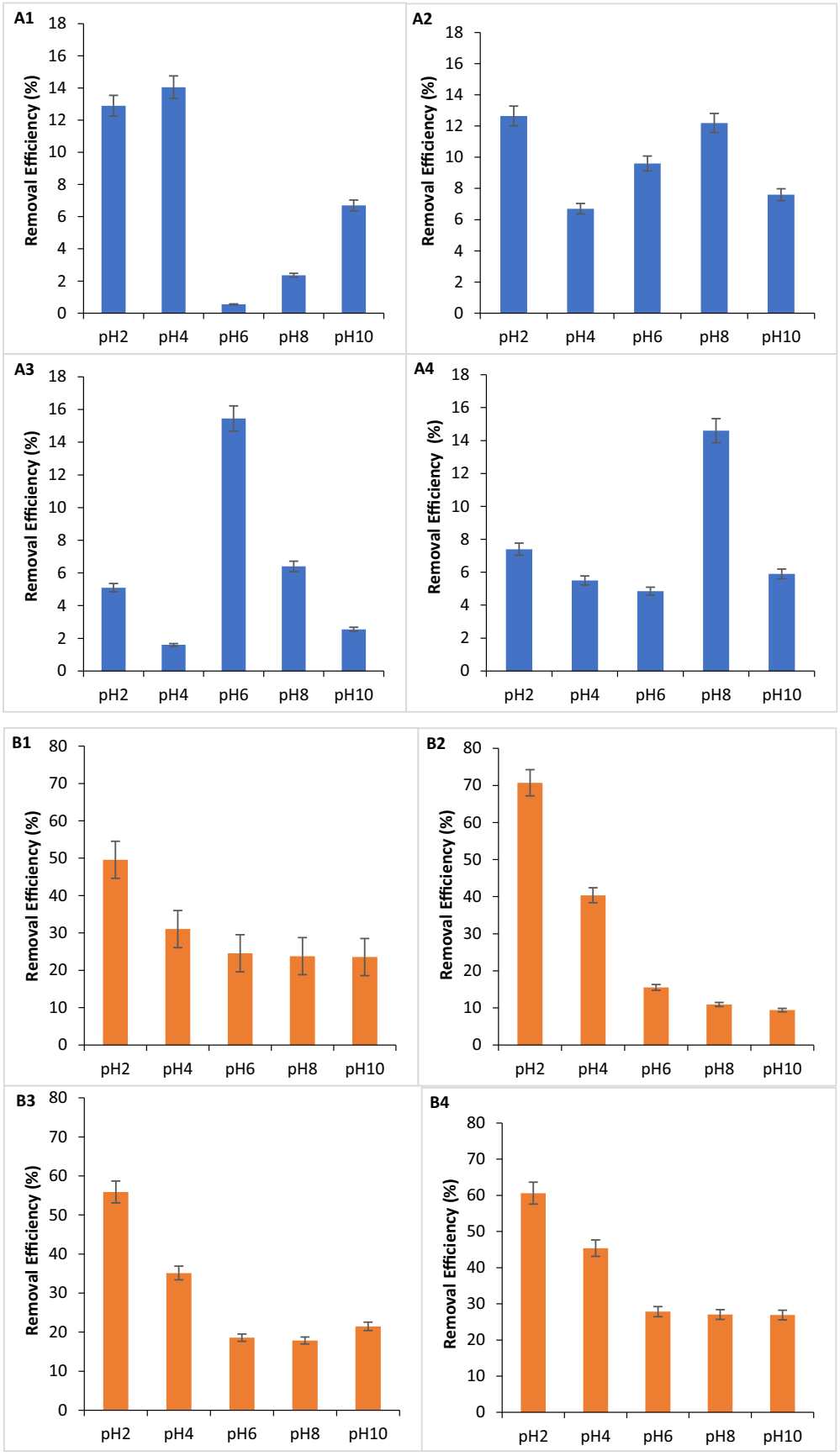

Fig. 2. A. Effect of pH on Li adsorption using (A1) activated carbon, (A2) bentonite, (A3) RDPs, and (A4) MDPs; B. Effect of pH on Mo adsorption using (B1) activated carbon, (B2) bentonite, (B3) RDPs, and (B4) MDPs.

the changes in pH value and can affect the speciation of the metal (Hawari et al., 2014).

3.2.2. Effect of pH on Mo adsorption

The results in Fig. 2B show clearly that the pH dependency of Mo removal is critical at the investigated pH values. Adsorbent's surface characteristics, as well as Mo species existing in water, can influence its adsorption process. In alkaline and neutral solutions, the H^+ ions concentration is very small, so the dominant Mo species are the monomeric Mo (VI) like $[MoO_4]^{2-}$ ions (Lee et al., 2011). As the pH is lowered, more H^+ ions are available and the anion molybdate species becomes protonated. Whether it polymerizes to hepta- or octa-molybdate depends on the pH and the Mo concentration, as at pH 5–6 the dominant species are hepta-molybdate ions $[Mo_7O_{24}]^{6-}$ and at pH 3–5, the dominant species is octa-molybdate ions $[Mo_8O_{26}]^4$ (Zhao et al., 2012). The neutral species H_2MoO_4 begins to form as the pH is further decreased. While in more acidic solutions, the concentration of hydrogen ions is high, so complexes with positive charge begin to form, and the $[MoO_2]^{2+}$ ions are the dominant species.

The decrease in adsorption with increasing pH value can be noticed from the obtained results, as it decreased from 49.57% to 23.54%, 70.72% to 9.41%, 55.9% to 21.94%, and 60.62% to 26.89% for AC, bentonite, RDPs, and MDPs, respectively. According to Sigworth and Smith (1972), the optimum adsorption of molybdenum occurs under acidic conditions, and it starts to decrease as the pH increases to 4.5. This can be attributed to the electrostatic attraction of Mo species $[MoO_2]^{2+}$ by the anion groups on the adsorbent surface. At higher pH, the adsorption of Mo decreased due to the competition for the adsorption sites between negatively charge molybdate species and hydroxyl ions (Zhao et al., 2012). Additionally, the negative charge molybdate species are electrostatically repulsed from the negative adsorption site. A similar favorable Mo adsorption with pH levels was found in other adsorbent studies. Tu et al. (2014) stated that the maximum Mo adsorption (30.59 mg/g) was found at pH 2.75. Similarly, Derakhshi et al. (2009) found that the maximum adsorption capacity of molybdenum by activated carbon was under pH 2 to 2.35.

3.3. Effect of initial adsorbate concentration on adsorption process

Fig. 3A shows the effect of Li initial concentration on the adsorption process using AC, bentonite, RDPs, and MDPs. The highest removal efficiency of Li was about 64% at 80 ppm using AC, followed by about 59% using MDPs at 50 ppm, about 35% at 20 ppm using bentonite, and about 25% at 20 ppm using RDPs. Moreover, the removal capacity was

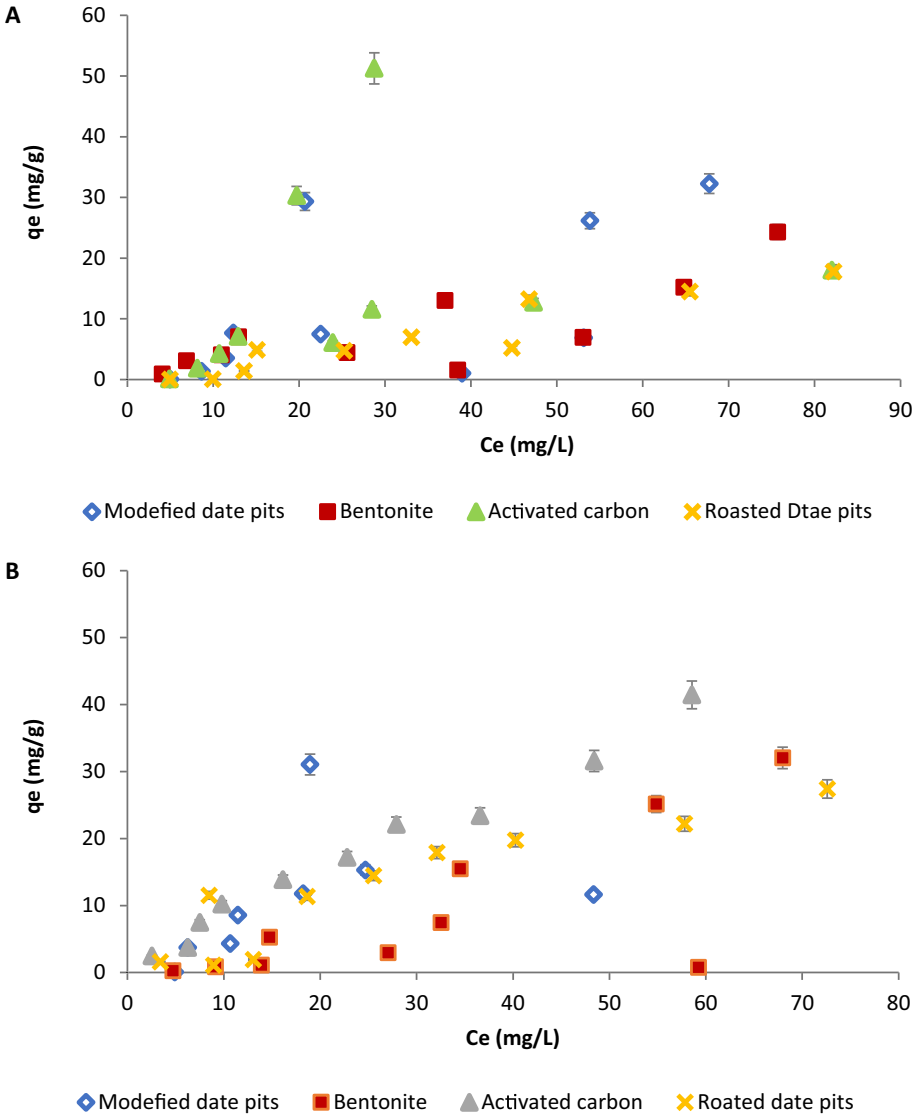

Fig. 3. Effect of initial concentration on the adsorption of (A) Li, (B) Mo.

increased with increasing the initial concentration, which would enhance the Li diffusion into pores. The decreasing of the adsorption efficiency at 100 ppm concentration could be related to the limited available vacant sites for adsorption, while the high adsorption capacity at low concentration could be due to the presence of unoccupied active adsorption sites. The obtained results were inconsistent with the results obtained by Al-Ghouti et al. (2019), as the concentration of mercury increases the adsorption capacity also increases on RDPs and sulfur-modified-RDPs. The heterogeneity of the adsorption process as well as the chemical binding could be the reason behind the fluctuating trend of increasing and decreasing Li removal efficiencies as the initial concentration increases. Furthermore, this can be explained by the availability of different oxygenated functional groups such as hydroxyl, ether, and carbonyl that considerably influence the adsorption mechanisms.

Fig. 3B shows the effect of the initial concentration of Mo on the adsorption process using AC, bentonite, RDPs, and MDPs. The highest removal efficiency of Mo was about 64% at 100 ppm using MDPs. Increasing the initial concentration led to increased adsorption, which indicates a positive correlation due to the availability of different adsorption mechanisms and more pores after the modification of date pits. While the highest removal efficiency of Mo was 58% using RDPs at 20 ppm, 51% at 20 ppm using AC, and 32% at 100 ppm using bentonite. It is shown that adsorption capacity increased with increasing initial concentration, due to the diffusion of Mo into the internal layer, besides the availability of various functional groups on the surface of the adsorbents. The decreasing adsorption efficiency at high concentrations is related to the limited availability of vacant adsorption sites. The high adsorption capacity at low concentrations could be attributed to the availability of unoccupied active adsorption sites.

3.4. Effect of temperature on adsorption process

Table 2 shows the effect of temperature on the adsorption of Li and Mo using AC, bentonite, RDPs, and MDPs. Fig. 4A shows the effect of temperature values 25 °C, 35 °C, and 45 °C on Li adsorption using AC, bentonite, RDPs, and MDPs. Overall, the adsorption efficiency of Li increases at 35 °C using the four adsorbents. At 35 °C, the maximum adsorption efficiency reached 95% for AC, 94% using MDPs, 63% using bentonite, and 38% using RDPs. Similar results were found by Al-Absi et al. (2022), who found that the removal of lithium by roasted date pits and its modification increased with increasing the temperature from 25 °C to 35 °C. The increase of adsorption efficiency with temperature is attributed to the increase of viscosity that enhances the mobility of metals. In addition to the swelling effect that facilitates the intra-particle diffusion and enables metals to further enter the internal pores hence increasing the adsorption capacity. While the removal efficiency decreases at 45 °C due to the high kinetic energy and mobility of Li that cause a collision and prevent it from adsorption to active adsorption sites. Similarly, Wahib et al. (2022) investigated the removal of lithium from groundwater by date pits and found that increasing the temperature had no significant effect on adsorption capacity. Another reason for decreasing the adsorption is that high temperatures could break down the adsorption bonds with active cites. At 45 °C, the maximum adsorption efficiency reached 86% for AC, 83% using MDPs, 57% using bentonite, and 29% using RDPs. This is supported by the BET results, which showed that AC shows the highest surface area of 178.79 m^2/g while RDPs show the lowest surface area of 2.84 m^2/g. The fluctuation trend of increasing and decreasing adsorption capacity indicates the possibility of reversible adsorption and different diffusion mechanisms such as intra-particle diffusion and complex formation (Al-Ghouti et al., 2010; Al-Ghouti et al., 2017). Besides, the fluctuation trend of increasing and decreasing adsorption capacity indicates that intra-particle diffusion governed the adsorption process more than the external diffusion (Hawari et al., 2014).

Table 2
Effect of solution temperature on Li and Mo adsorption onto different adsorbents.

Adsorbent	Li removal efficiency %		
	25 °C	35 °C	45 °C
AC	64.07	95.16	86.42
Bentonite	35.24	63.83	57.90
RDPs	24.51	38.04	29.19
MDPs	58.66	94.17	83.43

Adsorbent	Mo removal efficiency %		
	At 25 °C	At 35 °C	At 45 °C
AC	51.01	48.05	39.60
Bentonite	32.04	32.20	32.55
RDPs	57.60	49.60	47.49
MDPs	64.33	38.55	49.40

Fig. 4B shows the effect of temperature values 25 °C, 35 °C, and 45 °C on Mo adsorption using AC, bentonite, RDPs, and MDPs, respectively. Unlike lithium adsorption, increasing the temperature from 25 °C, to 35 °C, to 45 °C showed a decrease in the removal efficiency of molybdenum by the four studied adsorbents, which could mean that temperature is not a major contributing factor in this case. This could be attributed to the mobility of Mo that could prevent it from adsorption at active adsorption sites. At 45 °C, the adsorption efficiency decreased to 40% for AC and 47% using RDPs. While the adsorption efficiency decreases at 35 °C using the MDPs and bentonite adsorbents. The maximum adsorption efficiency reached 38% using MDPs and 32% using bentonite. It can be concluded that since lithium and molybdenum adsorption does not require high temperature, therefore, it does not require any additional energy or cost. Furthermore, this proves the effectiveness of the used adsorbents, as they are physically active at low temperatures.

3.5. Adsorption isotherm models

Adsorption isotherm models use the equilibrium data that is reached after the adsorbate moves to the solid phase from the liquid phase in which the adsorbent-adsorbate interaction at constant temperature can be described by the obtained equilibrium data (Al-Ghouti and Da'ana, 2020). The linear adsorption isotherms for Li and Mo adsorption onto bentonite, AC, RDPs, and MDPs at various temperatures (25 °C, 35 °C, and 45 °C) were investigated. Various isotherm models were used to investigate their applicability in the equilibrium data such as Langmuir and Freundlich models, while the energy parameters were estimated by using Dubinin-Radushkevich and Temkin. It was found that the Langmuir model describes well the adsorption of Li by bentonite at 45 °C ($R^2 = 0.88$ and $\chi^2 = 13$) as shown in Fig. 4. Similar results were obtained by Jiang et al. (2019), who studied the adsorption of lithium by lithium-aluminum adsorbent and found that Langmuir is the best fit model that describes the experimental data. Furthermore, Wang et al. (2017) investigated the removal of lithium by titanium type lithium-ion sieve and found that the adsorption of lithium followed the Langmuir isotherm model. According to the Langmuir model, monolayer uptake of Li occurred in these experiments. This indicates homogenous adsorption in which the adsorption energies are uniform. Langmuir adsorption constant (b) is associated with the increased attraction between the adsorbate and adsorbent; the high b value suggested the presence of strong binding while the lower b values suggest the lower binding as shown in Fig. 4.

Whereas, the non-fitted plot of Langmuir model Li adsorption using AC, RDPs, and MDPs showed two different linear lines; one line is at low concentrations, and the other is at high concentrations. This indicates the heterogeneous adsorption in which the highest adsorption energy sites are adsorbed first, and then the second adsorption energies are created allowing more adsorption at high concentrations. The creation

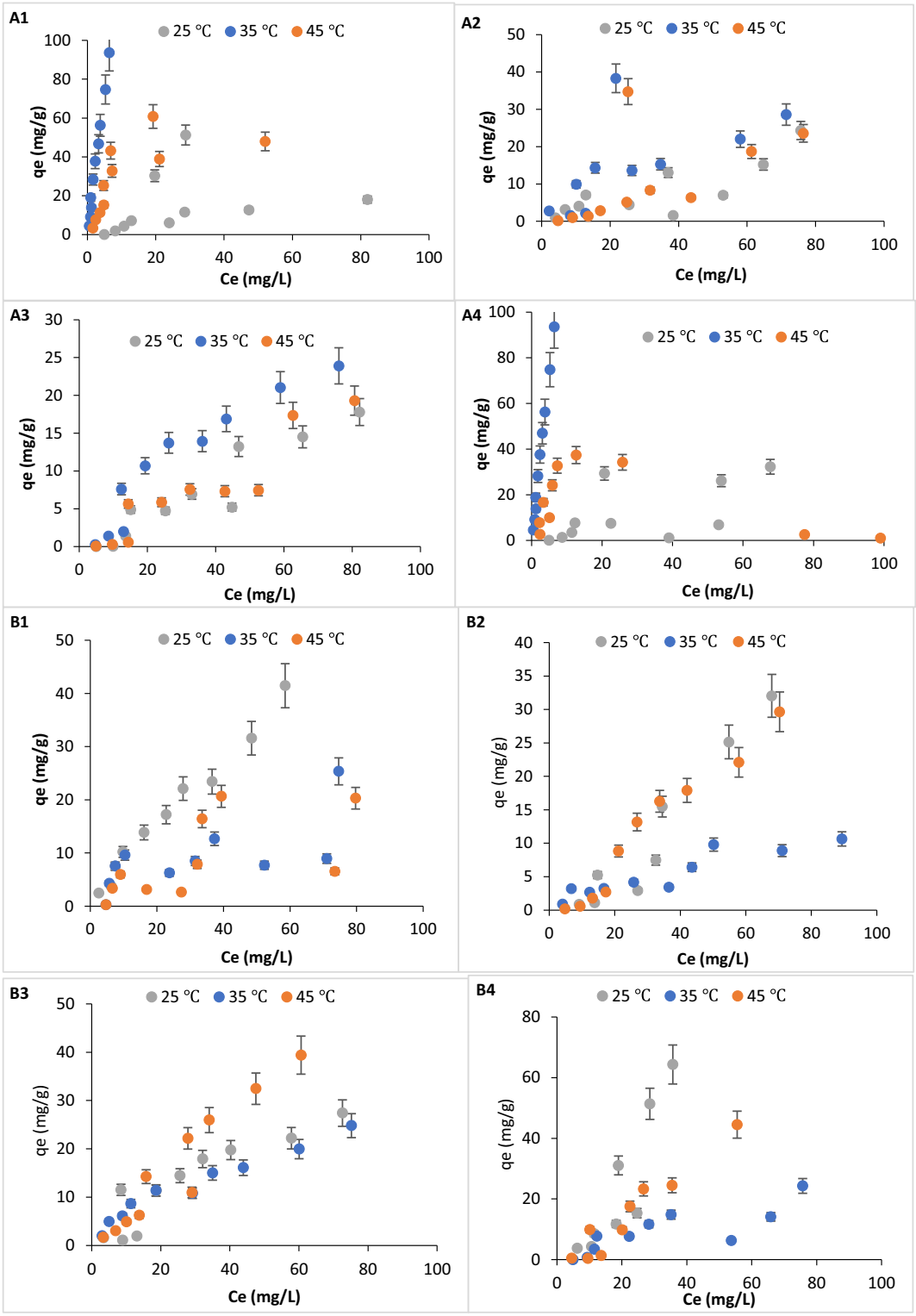

Fig. 4. A. Effect of different temperatures (25 °C, 35 °C, 45 °C) on Li adsorption onto (A1) activated carbon, (A2) bentonite, (A3) RDPs, and (A4) MDPs; B. effect of temperature on Mo adsorption using (B1) activated carbon, (B2) bentonite, (B3) RDPs, and (B4) MDPs, and Langmuir model, the best-fit model for lithium adsorption at 45 °C by different adsorbents (C1) AC, (C2) bentonite, (C3) RDPs, and (C4) MDPs.

of the second adsorption site is explained by the high concentration of adsorbate that creates pressure on the adsorbent surface and forces the adsorbates into the internal surface and pores. In addition, it could be explained by the formation of new adsorption sites due to the pressure force that removes blocks that hinder the adsorbates from entering the pores (Al-Ghouti et al., 2010). The interaction between both the adsorbent and adsorbate as well as the adsorption heat can be determined from the Temkin model as it assumes that the adsorption heat affects the adsorbate concentration, which is linearly decreased with the layer coverage onto a heterogeneous surface. The other assumption is

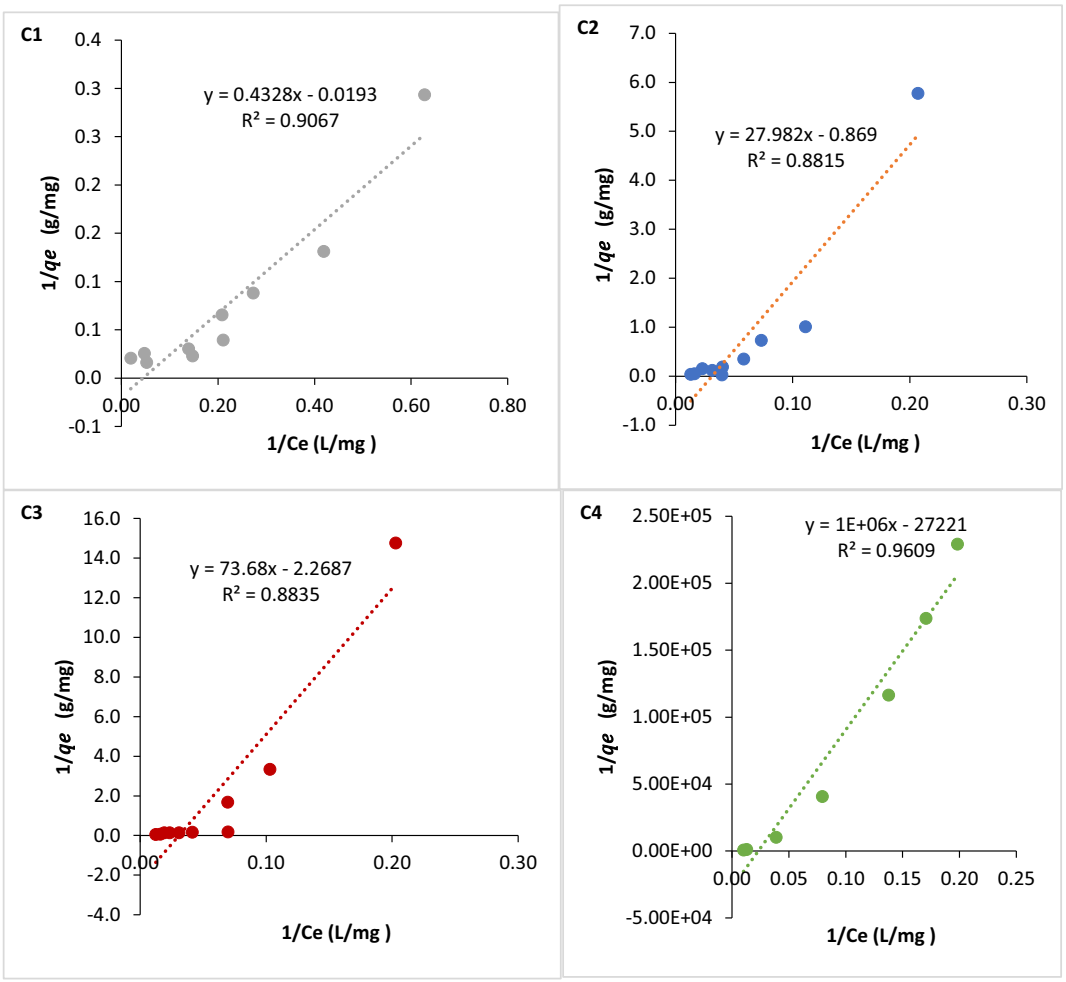

Fig. 4. (*continued*).

that the adsorption binding energies are uniformly distributed until it reaches maximum binding energy. The equilibrium-binding constant of the Temkin model is denoted as A_T (L/g), while the adsorption heat constant is denoted as RT/b_T (J/mol). It can be indicated from the decrease of adsorption heat with increasing the temperature that the adsorption process is exothermic. As can be seen from the results represented in Tables 3A and 3B, more than one isotherm model can be applicable for different adsorbents based on the R^2 value. However, the R^2 value is sensitive to outliers, which could mislead in fitting the model. Thus, χ^2 is also used for the determination of the good fit model. Temkin isotherm model is the best fit to describe the adsorption of Li by AC at 35 °C ($R^2 = 0.93$ and $\chi^2 = 9.5$), and at 45 °C ($R^2 = 0.75$ and $\chi^2 = 23$), by RDPs at 25 °C ($R^2 = 0.80$ and $\chi^2 = 4.3$), at 35 °C ($R^2 = 0.93$ and $\chi^2 = 0.7$), and at 45 °C ($R^2 = 0.75$ and $\chi^2 = 6.8$), by MDPs at 35 °C ($R^2 = 0.91$ and $\chi^2 = 8.4$). The Dubinin-Radushkevich model is temperature-dependent and the value of low mean free energy (E) indicates physisorption. Dubini-Radushkevich isotherm model is the best fit to describe the adsorption of Mo at 35 °C by MDP ($R^2 = 0.92$). Furthermore, Freundlich isotherm model describes well the adsorption Li by AC at 35 °C ($R^2 = 0.95$ and $\chi^2 = 9.2$), by MDPs at 35 °C ($R^2 = 0.98$ and $\chi^2 = 5.4$). According to the Freundlich model, multilayer uptake Li occurred in these experiments, which indicates heterogeneous adsorption energy. Thus, both chemisorption and physisorption are proposed adsorption mechanisms. It is also noticed that the values of the Freundlich adsorption constant (K_f) increase with increasing the temperature to 35 °C; While it decreased when the temperature increases to 45 °C. From the obtained results, the *n* value near one indicates a homogeneous surface.

3.6. Thermodynamic studies

From Table 4, the adsorption of Li and Mo onto AC and MDPs at 35 °C and 45 °C showed negative values for ΔG° that increased with increasing the temperature. This indicates the spontaneity and favorability of the adsorption process. However, the adsorption process was inferred to be endothermic due to the positive ΔH° value and the magnitude of ΔH° from 150 kJ/mol to 180 kJ/mol indicates that the adsorption mechanism between the adsorbate and adsorbent could be electrostatic interaction. Moreover, from the positive values of the entropy, it can be suggested that some structural changes can occur as well as readjustments in the adsorbent and adsorbate, which forms an active complex. Finally, (TΔS°) contributes more than ΔH°, thus the adsorption is an entropy-controlled process.

3.7. Adsorption experiments of real groundwater samples

Three real groundwater samples were used to study the adsorption of Li and Mo using AC, bentonite, RDPs, and MDPs. The effect of temperature was also studied at 25 °C as shown in Fig. 5A and C, and at 35 °C as shown in Fig. 5B and D. The concentrations of Li and Mo on the three studied groundwater samples are shown in Table 5. Li adsorption decreased with the increase in Li concentration due to competing with the other contaminants on the active sites. The percent of Li removal is the same for all adsorbents as the Li percentage removal reached only

Table 3A
Adsorption isotherm parameters of Li using different adsorbents.

Model	Temperature	Parameter	AC	Bentonite	RDPs	MDPs
Langmuir	25	Q_o (mg/g)	−0.54	14.61	−0.18	−0.28
		b (L/mg)	−0.043	0.021	−0.029	−0.040
		R^2	0.69	0.583	0.87	0.67
		X^2	102	49	205	261
	35	Q_o (mg/g)	−49	8.86	−1.7	−59
		b (L/mg)	−0.18	0.151	−0.033	−0.15
		R^2	0.91	0.206	0.84	0.97
		X^2	936	256	53	105
	45	Q_o (mg/g)	−51	−1.15	−0.440	-3.6×10^{-05}
		b (L/mg)	−0.044	−0.031	−0.030	−0.027
		R^2	0.90	0.881	0.883	0.96
		X^2	792	13	108	42,286
Freundlich	25	$1/n$	1.58	0.72	2.2	1.5
		K_f (mg/g) (L/mg)$^{1/n}$	0.060	0.55	0.0016	0.037
		R^2	0.58	0.51	0.80	0.48
		X^2	257	25	41	201
	35	$1/n$	1.1	0.81	1.5	1.1
		K_f (mg/g) (L/mg)$^{1/n}$	12	0.92	0.061	12
		R^2	0.94	0.54	0.840	0.97
		X^2	9.2	78	27	5.4
	45	$1/n$	0.74	1.70	1.9	0.87
		K_f (mg/g) (L/mg)$^{1/n}$	4.97	0.020	0.006	3.3
		R^2	0.72	0.80	0.84	0.62
		X^2	69	190	30	362
Dubini-Radushkevich	25	q_s (mg/g)	18	7.8	6.1	12
		K (mol^2/kJ^2)	-3×10^{-05}	-7×10^{-06}	-3×10^{-02}	-3×10^{-05}
		R^2	0.89	0.46	0.72	0.733
		X^2	119	54	–	119
	35	q_s (mg/g)	61	24	13	57
		K (mol^2/kJ^2)	-4×10^{-07}	-3×10^{-05}	-2×10^{-02}	-4×10^{-07}
		R^2	0.81	0.63	0.83	0.76
		X^2	34	45	–	118
	45	q_s (mg/g)	39	9.3	7.1	55
		K (mol^2/kJ^2)	-2×10^{-06}	-2×10^{-05}	-2×10^{-02}	−0.0025
		R^2	0.86	0.70	0.73	0.74
		X^2	88	137	–	–
Temkin	25	B (J/mol)	8.63	5.1	6.2	8.4
		b_t	286	483	398	294
		At (L/mg)	0.26	0.21	0.12	0.18
		R^2	0.21	0.48	0.79	0.35
		X^2	105	25	4.3	63
	35	B (J/mol)	34	7.9	9.0	34
		b_t	72	311	274.94	72
		At (L/mg)	1.58	0.36	0.158	1.52
		R^2	0.92	0.45	0.93	0.91
		X^2	9.5	34	0.7	8.4
	45	B (J/mol)	15	7.1	6.405	13
		b_t	160	346	386.96	179
		At (L/mg)	0.89	0.11	0.123	0.77
		R^2	0.74	0.62	0.75	0.75
		X^2	23	98	6.8	124

9% in groundwater sample 3. The adsorption of Li increased with increasing the temperature to 35 °C due to the mobility of adsorbate, which rearrange the adsorption process and allowed more Li to adsorb. All adsorbents, namely MDPs, RDPs, AC, and bentonite showed the same maximum percent of Li removal that reached 19% in groundwater sample 3.

In general, MDPs showed the highest adsorption of Mo in all GW samples. The adsorption of Mo increased with the increase in Mo concentrations, and the maximum Mo removal at 25 °C is 80% in sample 1 followed by 78% in sample 3 by using MDPs followed by RDPs, bentonite, and AC, with 75%, 71%, and 68% of Mo removal respectively. The adsorption of Mo increases with the increase in the temperature, and the maximum removal of Mo at 35 °C reached 92% in sample 3 and 80% in sample 2 using MDPs. This was followed by AC with 75% of Mo removal in sample 3, then 73% of Mo removal in sample 1 has the lowest Mo concentration using MDPs and RDPs, and 71% of Mo removal using bentonite in sample 3. Lithium adsorption from real groundwater and synthetic lithium chloride solution showed a similar trend in terms of temperature in which increasing the temperature caused a decrease in the removal efficiency of the four used adsorbents. However, the molybdenum removal efficiency increased with increasing the temperature, which also supports the obtained results from the synthetic solution.

3.8. Statistical analysis

A single-factor ANOVA test was used to test the pH effect on Li and Mo adsorption using AC, bentonite, RDPs, and MDPs. It was found that the p-value ≥ 0.05 and F value $< F_{Critical}$, which means that the difference was not significant, and the null hypothesis was accepted. Furthermore, the relationship between concentration and temperature of both metals was tested by two-way ANOVA and the results showed that the null hypothesis was rejected due to the highly significant difference since the p-value ≤ 0.05 and F-value $> F_{Critical}$. In addition, there is a highly significant difference between the adsorbents, namely AC, bentonite, RDPs, and MDPs as the F-value $> F_{Critical}$, and p-value ≤ 0.05. Moreover, the two-way ANOVA test showed a highly significant difference between Mo concentration and temperature in the adsorption

Table 3B
Adsorption isotherm parameters of Mo using different adsorbents.

Model	Temperature	Parameter	AC	Bentonite	RDPs	MDPs
Langmuir	25	Q_o (mg/g)	74	−5.133	45	−71
		b (L/mg)	0.013	−0.012	0.010	−0.0076
		R^2	0.93	0.782	0.64	0.78
		X^2	4.8	90	39	157
	35	Q_o (mg/g)	−3.3	15.197	21	−0.28
		b (L/mg)	−0.023	0.018	0.037	−0.038
		R^2	0.44	0.839	0.94	0.72
		X^2	170	3.8	12	290
	45	Q_o (mg/g)	−2.9	−1.266	−100	0.58
		b (L/mg)	−0.026	−0.030	−0.005	−14
		R^2	0.60	0.944	0.978	0.62
		X^2	50	34	10	598
Freundlich	25	$1/n$	0.89	1.78	1.04	1.1
		K_f (mg/g)(L/mg)$^{1/n}$	1.05	0.017	0.36	0.53
		R^2	0.96	0.90	0.67	0.52
		X^2	1.9	34	29	123
	35	$1/n$	0.76	0.67	0.67	1.6
		K_f (mg/g) (L/mg)$^{1/n}$	0.62	0.49	1.34	0.023
		R^2	0.45	0.83	0.94	0.68
		X^2	30	3.2	1.7	54
	45	$1/n$	0.99	1.97	1.1	0.19
		K_f (mg/g) (L/mg)$^{1/n}$	0.24	0.010	0.39	0.72
		R^2	0.55	0.93	0.93	0.44
		X^2	41	22	8.7	2192
Dubini-Radushkevich	25	q_s (mg/g)	26	6.3	23	35
		K (mol^2/kJ^2)	-1×10^{-05}	-2×10^{-05}	-5×10^{-05}	-4×10^{-05}
		R^2	0.88	0.46	0.89	0.53
		X^2	213	54	6.5E06	173
	35	q_s (mg/g)	12	24	13	12
		K (mol^2/kJ^2)	-1×10^{-05}	-3×10^{-05}	-4×10^{-06}	-3×10^{-05}
		R^2	0.70	0.66	0.79	0.91
		X^2	24	10	15	9997
	45	q_s (mg/g)	10	11	16	0.72
		K (mol^2/kJ^2)	-1×10^{-05}	-2×10^{-05}	-5×10^{-06}	−0.19
		R^2	0.69	0.71	0.58	0.44
		X^2	37	61	74	–
Temkin	25	B (J/mol)	11	14	8.6	27
		b_t	213	166	285	89
		At (L/mg)	0.27	0.081	0.22	0.14
		R^2	0.87	0.78	0.81	0.67
		X^2	6	15	10	71
	35	B (J/mol)	0.43	2.9	6.2	6.6
		b_t	596	853	396.70	370
		At (L/mg)	4.1	0.25	0.360	0.17
		R^2	0.42	0.76	0.91	0.68
		X^2	60	8.12	7.6	12.7
	45	B (J/mol)	5.21	11	13.03	1.6
		b_t	474	217	190.26	1469
		At (L/mg)	0.23	0.11	0.189	0.11
		R^2	0.44	0.87	0.80	0.49
		X^2	25	0.97	2.8	1120

experiment using GW samples as the F-value $>$ $F_{Critical}$, and p-value $\leq$ 0.05, thus the null hypothesis of equal means was rejected.

3.9. Comparative adsorption study

Table 6 shows the comparison of Li and Mo adsorption respectively in different solutions such as single adsorbate solution, and real GW solution at 25 °C. The adsorption of Li decreases in real GW solutions than the adsorption from Li solution only because Li concentration in real GW is very low. Besides, Li ions could not compete with the other ions present in the solution at the active sites. Thus, the electrostatic interactions between the adsorbate and adsorbent can be affected by the solution ionic strength (Wong et al., 2003).

The adsorption capacity of Mo from the solution that contains 5 ppm Mo was the highest by using MDPs (80% of removal). The adsorption of Mo increases significantly in real GW solutions than the adsorption in Mo solution because Mo concentration in GW is very low and Mo ions have a higher capacity to adsorb onto the active sites than other ions. This indicates that the adsorption of Mo onto MDPs surface has various adsorption mechanisms such as electrostatic interaction, ion change, and complex formation onto the active sites, besides possible intra-diffusion into pores.

Mo does not form simple ions in an aqueous solution; while Li forms Li^+ cations. In a slightly alkaline aqueous solution, the dominant Mo species are molybdate anions MoO_4^{2-} as +6 is the most stable oxidation state for Mo. Date pits consist of about 17.5% hemicellulose, 11.0% lignin, and 42.5% cellulose (Al-Ghouti et al., 2010). Oxygenated functional groups exist due to the presence of cellulose and hemicellulose (Hawari et al., 2014). This is supported by the FTIR results (figure not shown) that showed the availability of the different oxygenated functional groups such as hydroxyl groups in the range of 3356 cm^{-1}–3560 cm^{-1}, carboxyl at 1744 cm^{-1}, and thiol groups at 1374 cm^{-1} that indicate the possibility of chemical adsorption mechanisms besides the physical adsorption. Similarly, MDPs have oxygenated functional groups such as the carbonyl group in addition to the peak around 1703 cm^{-1} representing the mercapto-acetate functions with the thiol groups. Physical adsorption is supported by the physical analysis results using BET as shown in Table 1, respectively. That showed the high surface area

Table 4
Thermodynamic parameters of Li and Mo adsorption onto different adsorbents.

Adsorbent	Temperature °C	ln *b* or ln K_f*	ΔG° (kJ/mol)	ΔH° (kJ/mol)	ΔS° (J/mol·K)
Li					
AC	25	−2.8	4.5	180	580
	35	2.5	−1.3		
	45	1.6	−7.0		
Bentonite	25	−3.9	8.0	−0.22	−28
	35	−1.9	8.3		
	45	−4.0	8.5		
RDPs	25	−6.4	14	55	140
	35	−2.8	12		
	45	−5.1	11		
MDPs	25	−3.2	5.4	181	590
	35	2.5	−0.47		
	45	1.2	−6.4		
Mo					
AC	25	−4.4	8.9	120	360
	35	−0.47	5.2		
	45	−1.4	1.6		
Bentonite	25	−4.0	9.8	−18	−93
	35	−4.0	11		
	45	−4.5	12		
RDPs	25	−4.6	12	144	444
	35	−3.3	7.4		
	45	−0.93	3.0		
MDPs	25	−0.63	4.2	10	19
	35	−3.8	4.0		
	45	−0.31	3.8		

* Langmuir isotherm constant (*b*) or Freundlich isotherm constant (K_f) depend on the applicability of the models.

Table 5
The concentration of Li and Mo on the three studied GW samples.

	Initial concentration C_o (μg/L)	
	Mo	Li
Groundwater sample 1	75	209
Groundwater sample 2	77	465
Groundwater sample 3	142	99

Table 6
Comparative study for Li and Mo adsorption at 25 °C.

Adsorbent	Li removal efficiency %	
	Li solution (5 ppm Li)	Real GW (0.465 ppm)
AC	19	9
Bentonite	19	7
RDPs	10	7
MDPs	14	9

Adsorbent	Mo removal efficiency %	
	Mo solution (5 ppm)	Real GW (0.143 ppm)
AC	49	68
Bentonite	8	27
RDPs	32	73
MDPs	37	80

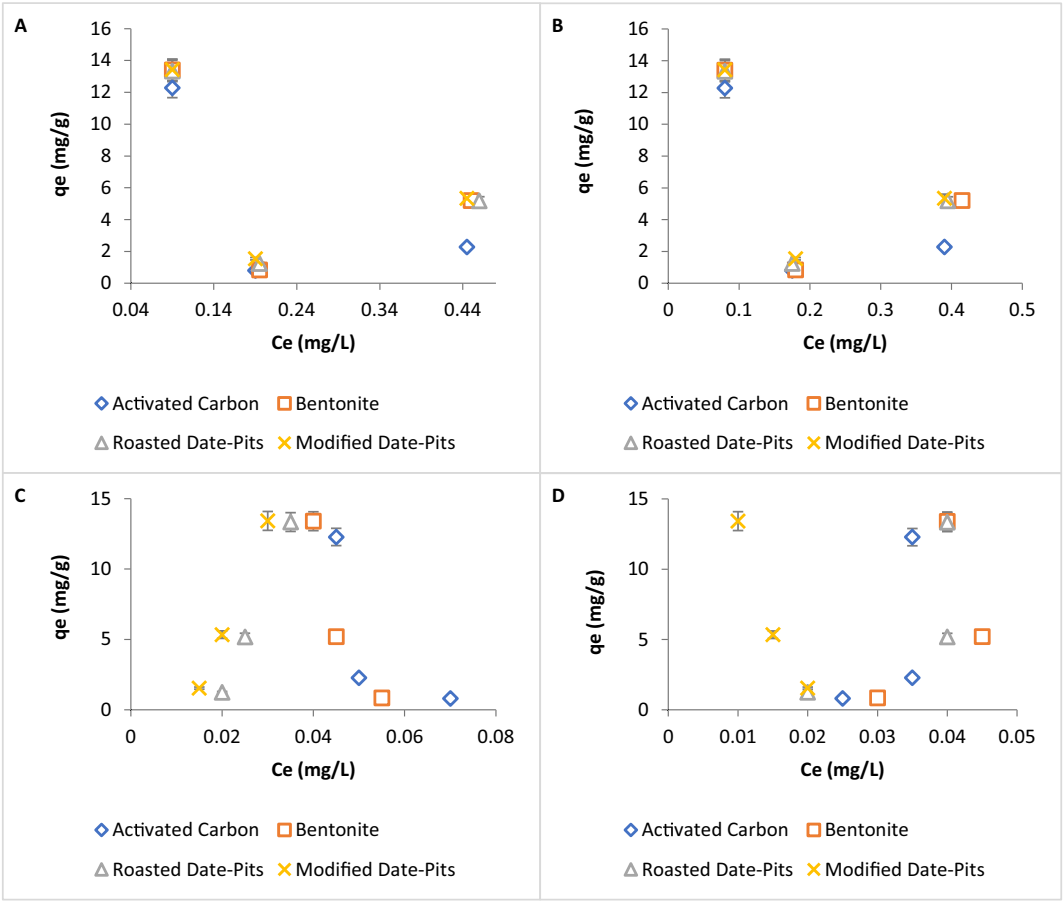

Fig. 5. Li and Mo adsorption from real groundwater samples at (A) Li adsorption at 25 °C, (B) Li adsorption at 35 °C, (C) Mo adsorption at 25 °C, (D) Mo adsorption at 35 °C.

and the pores volume of AC and MDPs adsorbents that enhanced the adsorption capacity of lithium and molybdenum from real GW samples. While the availability of the negative active functional groups indicates chemical adsorption mechanisms such as hydrogen bond, electrostatic complexation, and/or interaction. Thus, the proposed adsorption mechanisms onto MDPs active sites are van der Waal's, electrostatic interaction, hydrogen bond, and/or complexation. This is supported by the thermodynamic results that the adsorption of Li on AC and MDPs at 35 °C and 45 °C showed negative values for free energy ΔG° that is increased for higher temperature, while the magnitude of ΔH° from 150 to 180 kJ/mol indicates electrostatic interaction and chemical adsorption.

In an alkaline solution, deprotonation of carboxylic and phenolic functional groups occurs, and the surface charge became negatively charged. Thus, Li^+ cations electrostatically interact with the negative functional groups. Also, Li^+ could interact with borate ions because Li is an alkali earth metal that forms metallic complexes such as $[Li\ B(OH)_4]^+$, and $[Li_2\ MoO_4]^{2+}$. Al-Ghouti and Salih (2018) showed that in the basic environment, $[Mg\ B(OH)_4]^+$ is formed due to the reaction between borate and magnesium ions. On the other hand, MoO_4^{2-} and $B(OH)_4^-$ anions are repelled with negatively charged functional groups. Shan et al. (2012) showed that MoO_4^{2-} adsorbed by ion exchange with hydroxyl ions or neutral water molecules available in the solution around the adsorbent that is made from orange peels. Thus, the proposed mechanisms for MoO_4^{2-} and $B(OH)_4^-$ adsorption is when cellulose and/or lignin capture free proton during the complexing of borate and molybdate by functional groups such as hydroxyl which then interact with borate ion through a covalent attachment and form a coordination complex as shown in Fig. 6A and B. A similar mechanism is shown by Wolska and Bryjak (2013) that described the formation of mono-, di, and tri coordination of boron complexation by a tertiary amine group. The possible surface complexation (mono-, di-, and tri-coordination) onto MDPs between surface hydroxyls (XOH) and adsorbate ions (A) such as Li^+ cations (A^+), and MoO_4^{2-} and $B(OH)_4^-$ anions (A^-) are described in reaction Eqs. 3, 4, 5, and 6.

$$XOH_{(s)} + H^+_{(aq)} \longleftrightarrow XOH^+_{2(s)} \quad (3)$$

$$XOH^+_{2(s)} \longleftrightarrow XO^-_{(aq)} + H^+_{(aq)} \quad (4)$$

$$XO^-_{(aq)} + A^+_{(aq)} \longleftrightarrow XA_{(s)} \quad (5)$$

$$XOH^+_{2(s)} + A^-_{(aq)} + H^+_{(aq)} \longleftrightarrow XA_{(s)} + H_2O \quad (6)$$

Furthermore, the intra-diffusion within the pores is also proposed as SEM and BET results showed the high surface area and the pores volume for the adsorbents that enhanced the removal efficiency as shown in Fig. 6 and Table 1, respectively. In addition, Mo has Pauling electronegativity higher than Li electronegativity thus, it adsorbs on the surface more readily. After that it could migrate into the pores, however, the high electronegativity may hinder them from migrating into the pores and keeping them adsorb onto the surface. While the lower ionic radius and hydration radius for Li than for Mo indicated that Li has the ability for external and internal adsorption because Li could migrate into the pores easier than Mo. Another parameter that affects the adsorption is that Li is a strongly hydrated ion while $B(OH)_4^-$ is neither that of a strongly hydrated ion nor that of hydrophobic ions (Corti et al., 1980). It is also indicated from the fluctuation trend of increasing and decreasing adsorption capacity indicates that intra-particle diffusion governed the adsorption process more than the external diffusion.

4. Conclusion

To conclude, results showed that pH 6 as the optimum pH influences the interaction between the adsorbent's surface and the adsorbate's ions. Additionally, the adsorption process by MDPs was favorable indicating that the adsorption process is spontaneous and endothermic. FTIR analysis confirmed the presence of different oxygenated functional groups that are responsible for adsorbates adsorption onto MDPs. Hence, this study proved that MDPs are valuable for remediating Li and Mo from GW. The negative values for free energy indicate a spontaneous and favorable adsorption process at high temperatures. The positive entropy values indicate that the adsorbent-adsorbate complex might have undergone some readjustments or structural changes.

CRediT authorship contribution statement

Ayesha Y. Ahmad: Formal analysis, Methodology, Validation, Writing – review & editing. **Mohammad A. Al-Ghouti:** Conceptualization, Supervision, Visualization, Methodology, Validation, Writing –

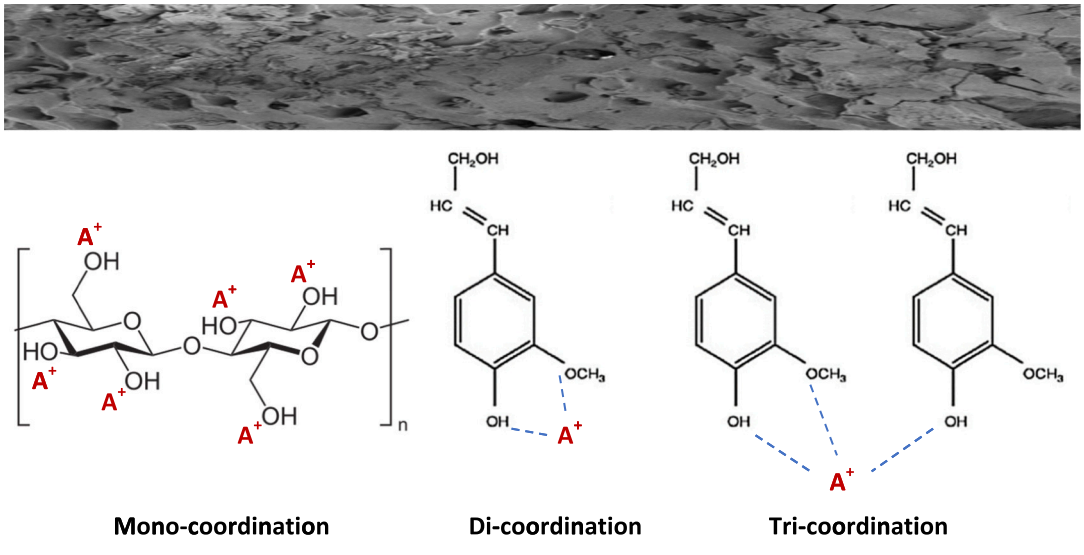

Fig. 6. Schematic diagram of adsorption onto (A) cellulose structure, (B) phenylpropanoid units found in lignin.

review & editing. **Majeda Khraisheh:** Methodology, Validation, Writing – review & editing. **Nabil Zouari:** Methodology, Validation, Writing – review & editing.

Declaration of competing interest

The authors declare that they have no known competing financial interests or personal relationships that could have appeared to influence the work reported in this paper.

Acknowledgment

This publication was made possible by NPRP grant # [12S-0307-190250] from the Qatar National Research Fund (a member of Qatar Foundation). The findings achieved herein are solely the responsibility of the author[s]. Thanks to Ms. Dana Da'na for editing the final version of the manuscript. The ICP-MS analysis was accomplished in the Central Laboratories Unit, Qatar University.

References

Ahmad, A.Y., Al-Ghouti, M.A., Khraisheh, M., Zouari, N., 2020. Hydrogeochemical characterization and quality evaluation of groundwater suitability for domestic and agricultural uses in the state of Qatar. Groundw. Sustain. Dev. 11, 100467 https://doi.org/10.1016/j.gsd.2020.100467.

Ahmad, T., Danish, M., Rafatullah, M., Ghazali, A., Sulaiman, O., Hashim, R., Ibrahim, M.N., 2011. The use of date palm as a potential adsorbent for wastewater treatment: a review. Environ. Sci. Pollut. Res. 19 (5), 1464–1484. https://doi.org/10.1007/s11356-011-0709-8.

Al-Absi, R.S., Abu-Dieyeh, M.H., Ben-Hamadou, R., Nasser, M.S., Al-Ghouti, M.A., 2021. Novel composite materials of modified roasted date pits using ferrocyanides for the recovery of Li ions from seawater reverse osmosis brine. Sci. Rep. 11 (1), 1–17. https://doi.org/10.1038/s41598-021-98438-2.

Al-Absi, R., Abu-Dieyeh, M., Ben-Hamadou, R., Nasser, M., Al-Ghouti, M., 2022. Thermodynamics, isotherms, and mechanisms studies of lithium recovery from seawater desalination reverse osmosis brine using roasted and ferrocyanide modified date pits. Environ. Technol. Innov. 25, 102148 https://doi.org/10.1016/j.eti.2021.102148.

Al-Ghouti, M.A., Da'ana, D.A., 2020. Guidelines for the use and interpretation of adsorption isotherm models: a review. J. Hazard. Mater. 393, 122383 https://doi.org/10.1016/j.jhazmat.2020.122383.

Al-Ghouti, M.A., Salih, N.R., 2018. Application of eggshell wastes for boron remediation from water. J. Mol. Liq. 256, 599–610. https://doi.org/10.1016/j.molliq.2018.02.074.

Al-Ghouti, M., Al Disi, Z., Alkaabi, N., Khraisheh, M., 2017. Mechanistic insights into the remediation of bromide ions from desalinated water using roasted date pits. Chem. Eng. J. https://doi.org/10.1016/j.cej.2016.09.091.

Al-Ghouti, M.A., Da'ana, D., Abu-Dieyeh, M., Khraisheh, M., 2019. Adsorptive removal of mercury from water by adsorbents derived from date pits. Sci. Rep. 9 (1) https://doi.org/10.1038/s41598-019-51594-y.

Al-Ghouti, M.A., Li, J., Salamh, Y., Al-Laqtah, N., Walker, G., Ahmad, M.N., 2010. Adsorption mechanisms of removing heavy metals and dyes from aqueous solution using date pits solid adsorbent. J. Hazard. Mater. 176 (1–3), 510–520. https://doi.org/10.1016/j.jhazmat.2009.11.059.

Al-Shidi, F.K., 2014. Study the Quality of Groundwater of Al-Zoroup Area in Mahdah State, The Sultanate of Oman. United Arab Emirate University. Theses and Dissertations paper, 12. https://scholarworks.uaeu.ac.ae/all_theses/114.

Amin, M., Alazba, A., Shafiq, M., 2016. Adsorption of copper (Cu2+) from aqueous solution using date palm trunk fibre: isotherms and kinetics. Desalin. Water Treat. 57 (47), 22454–22466. https://doi.org/10.1080/19443994.2015.1131635.

Corti, H., Crovetto, R., Fernández-Prini, R., 1980. Properties of the borate ion in dilute aqueous solutions, 76 (0), 2179. https://doi.org/10.1039/f19807602179.

Daniel, C., Harris, W.H., 2011. Quantitative Chemical Analysis, eighth ed. Freeman.

Derakhshi, P., Ghafourian, H., Khosravi, M., Rabani, M., 2009. Optimization of molybdenum adsorption from aqueous solution using granular activated carbon. World Appl. Sci. J. 7 (2), 230–238.

El-Alfy, M., Lashin, A., Abdalla, F., Al-Bassam, A., 2017. Assessing the hydrogeochemical processes affecting groundwater pollution in arid areas using an integration of geochemical equilibrium and multivariate statistical techniques. Environ. Pollut. 229, 760–770. https://doi.org/10.1016/j.envpol.2017.05.052.

Etteieb, S., Cherif, S., Tarhouni, J., 2015. Hydrochemical assessment of water quality for irrigation: a case study of the Medjerda River in Tunisia. Appl Water Sci 7 (1), 469–480. https://doi.org/10.1007/s13201-015-0265-3.

Hawari, A., Khraisheh, M., Al-Ghouti, M.A., 2014. Characteristics of olive mill solid residue and its application in remediation of Pb2+, Cu2+ and Ni2+ from aqueous solution: mechanistic study. Chem. Eng. J. 251, 329–336. https://doi.org/10.1016/j.cej.2014.04.065.

Heibati, B., Rodriguez-Couto, S., Amrane, A., Rafatullah, M., Hawari, A., Al-Ghouti, M., 2014. Uptake of Reactive Black 5 by pumice and walnut activated carbon: Chemistry and adsorption mechanisms. J. Ind. Eng. Chem. 20 (5), 2939–2947. https://doi.org/10.1016/j.jiec.2013.10.063.

Huang, F., Yi, F., Wang, Z., Li, H., 2016. Sorptive removal of Ce(IV) from aqueous solution by bentonite. Procedia Environ. Sci. 31, 408–417. https://doi.org/10.1016/j.proenv.2016.02.073.

IMOA, 2018. Annual Review 2018/2019. International Mo Association.

Jiang, H., Yang, Y., Sun, S., Yu, J., 2019. Adsorption of lithium ions on lithium-aluminum hydroxides: equilibrium and kinetics. Can. J. Chem. Eng. 98 (2), 544–555. https://doi.org/10.1002/cjce.23640.

Karnib, M., Kabbani, A., Holail, H., Olama, Z., 2014. Heavy metals removal using activated carbon, silica and silica activated carbon composite. Energy Procedia 50, 113–120. https://doi.org/10.1016/j.egypro.2014.06.014.

Kuiper, N., Rowell, C., Shomar, B., 2015. High levels of Mo in Qatar's groundwater and potential impacts. J. Geochem. Explor. 150, 16–24. https://doi.org/10.1016/j.gexplo.2014.12.009.

Lee, M., Sohn, S., Lee, M., 2011. Ionic equilibria and ion exchange of Mo(VI) from strong acid solution. Bull. Kor. Chem. Soc. 32 (10), 3687–3691. https://doi.org/10.5012/bkcs.2011.32.10.3687.

Mallick, J., Singh, C., Almesfer, M., Kumar, A., Khan, R., Islam, S., Rahman, A., 2018. Hydro-geochemical assessment of groundwater quality in Aseer Region, Saudi Arabia. Water 10 (12), 1847. https://doi.org/10.3390/w10121847.

Nagul, E.A., Mckelvie, I.D., Worsfold, P., Kolev, S.D., 2015. The Mo blue reaction for the determination of orthophosphate revisited: opening the black box. Anal. Chim. Acta 890, 60–82. https://doi.org/10.1016/j.aca.2015.07.030.

Shafiq, M., Alazba, A.A., Amin, M.T., 2019. Synthesis, characterization, and application of date palm leaf waste-derived biochar to remove cadmium and hazardous cationic dyes from synthetic wastewater. Arab. J. Geosci. 12 (2) https://doi.org/10.1007/s12517-018-4186-y.

Shan, W., Fang, D., Zhao, Z., Shuang, Y., Ning, L., Xing, Z., Xiong, Y., 2012. Application of orange peel for adsorption separation of Mo(vi) from re-containing industrial effluent. Biomass Bioenergy 37, 289–297. https://doi.org/10.1016/j.biombioe.2011.11.015.

Shannon, R.D., 1976. Revised effective ionic radii and systematic studies of interatomic distances in halides and chalcogenides. Acta Crystallographica Section A 32 (5), 751–767. https://doi.org/10.1107/s0567739476001551.

Sigworth, E., Smith, S., 1972. Adsorption of inorganic compounds by activated carbon. J. Am. Water Works Assoc. 64 (6), 386–391. https://doi.org/10.1002/j.1551-8833.1972.tb02713.x.

Sun, D., Meng, M., Qiao, Y., Zhao, Y., Yan, Y., Li, C., 2018. Synthesis of ion imprinted nanocomposite membranes for selective adsorption of lithium. Sep. Purif. Technol. 194, 64–72. https://doi.org/10.1016/j.seppur.2017.10.052.

Tu, Y., You, C., Chang, C., Chan, T., Li, S., 2014. Xanes evidence of Mo adsorption onto novel fabricated nano-magnetic cufe2o4. Chem. Eng. J. 244, 343–349. https://doi.org/10.1016/j.cej.2014.01.084.

Wahib, S.A., Da'na, D.A., Zaouri, N., Hijji, Y.M., Al-Ghouti, M.A., 2022. Adsorption and recovery of Li ions from groundwater using date pits impregnated with cellulose nanocrystals and ionic liquid. J. Hazard. Mater. 421, 126657. https://doi.org/10.1016/j.jhazmat.2021.126657.

Wang, S., Li, P., Zhang, X., Zheng, S., Zhang, Y., 2017. Selective adsorption of lithium from high Mg-containing brines using H x TiO 3 ion sieve. Hydrometallurgy 174, 21–28. https://doi.org/10.1016/j.hydromet.2017.09.009.

Wang, Y., Weinstock, I.A., 2012. Polyoxometalate-decorated nanoparticles. Chem. Soc. Rev. 41 (22), 7479. https://doi.org/10.1039/c2cs35126a.

Wolska, J., Bryjak, M., 2013. Methods for boron removal from aqueous solutions- a review. Desalination 310, 18–24. https://doi.org/10.1016/j.desal.2012.08.003.

Wong, K.K., Lee, C.K., Low, K.S., Haron, M.J., 2003. Removal of Cu and Pb by tartaricacid modified rice husk from aqueous solution. Chemosphere. 50, 23–28.

Yadav, S.K., Singh, D.K., Sinha, S., 2013. Adsorption study of lead(ii) onto xanthated date palm trunk: kinetics, isotherm and mechanism. Desalin. Water Treat. 51 (34–36), 6798–6807. https://doi.org/10.1080/19443994.2013.792142.

Yang, S., Li, J., Lu, Y., Chen, Y., Wang, X., 2009. Sorption of NI(II) on gmz bentonite: Effects of pH, ionic STRENGTH, FOREIGN ions, humic acid and temperature. Appl. Radiat. Isot. 67 (9), 1600–1608. https://doi.org/10.1016/j.apradiso.2009.03.118.

Younas, F., Mustafa, A., Farooqi, Z., Wang, X., Younas, S., Mohy-Ud-Din, W., et al., 2021. Current and emerging adsorbent technologies for wastewater treatment: trends, limitations, and environmental implications. Water 13 (2), 215. https://doi.org/10.3390/w13020215.

Zhang, W., Mou, Y., Zhao, S., Xie, L., Wang, Y., Chen, J., 2017. Adsorption materials for Li ion from brine resources and their performances. Prog. Chem. 29 (2/3), 231–240. https://doi.org/10.7536/PC161012.

Zhao, Z., Xu, X., Chen, X., Huo, G., Chen, A., Liu, X., Xu, H., 2012. Thermodynamics and kinetics of adsorption of Mo blue with d301 ion exchange resin. Trans. Nonferrous Metals Soc. China 22 (3), 686–693. https://doi.org/10.1016/s1003-6326(11)61232-6.